ELSEVIER

International Journal of Heat and Fluid Flow 23 (2002) 96–104

International Journal of HEAT AND FLUID FLOW

www.elsevier.com/locate/ijhff

Free convective mass transfer at down-pointing truncated cones

J. Krýsa [a], A.A. Wragg [b,*], M.A. Patrick [b]

[a] *Department of Inorganic Technology, Institute of Chemical Technology, Technicka 5, l66 28 Prague 6, Czech Republic*
[b] *Department of Engineering, University of Exeter, North Park Road, Exeter EX4 4QF, UK*

Received 8 October 1999; accepted 29 July 2001

Abstract

Free convective mass transfer at down-pointing truncated cones was experimentally studied using the electrochemical limiting diffusion current technique. The total mass transfer coefficient has the same dependence on height as that of a conical surface; however, the values are higher because of the high mass transfer at the up-facing horizontal surface. The flow development after sudden switch on of the limiting current potential was observed. The flow begins as a ring of fluid rising from the upper cone periphery followed by necking of the plume and a steady-state situation arises in which there is a complex flow structure consisting of a multiplicity of close spaced interacting convection streams. The experimental total mass transfer data were correlated using a method which includes an interference factor taking account of the fact that the conical and up-facing horizontal surfaces of the truncated cones are exposed to fluid which has already been depleted in cupric ions as it flows up from the down-facing horizontal surface.

Keywords: Free convection; Mass transfer; Heat transfer; Truncated cone

1. Introduction

Knowledge of free convective heat transfer and, therefore, the prediction of heat losses from various objects of complex geometry is very important, for instance in design for heat dissipation from electronic components. Mass transfer measurements are known to provide good simulation of free convective heat transfer (Patrick and Wragg, 1985). The limiting diffusion current technique of mass transfer measurement is attractive as a cold modelling method for heat transfer since the measurements are usually simpler, cheaper and speedier than direct heat transfer measurements. Moreover, it is also easy to determine the heat transfer performance of the individual surfaces in a complex multi-surface geometry. The work of Worthington et al. (1987) on the mass transfer simulation of heat transfer at cuboid shapes was prompted by an industrial need for data concerning the passive cooling of electronic components. However such components may also be of cylindrical shape and of non-uniform cross-section and real devices may have surfaces which are inclined from the vertical. In this work therefore we turn attention to shapes with two horizontal surfaces and a varying diameter, the truncated cone, a good generic example of a 3-D body comprising several variously behaving individual surfaces.

This work continues previous studies devoted to free convective mass transfer at complex 3-D objects such as vertical cylinders (Krýsa and Wragg, 1992), up-pointing and down-pointing pyramids (Krýsa and Wragg, 1996, 1997). The down-pointing truncated cone is a case of a 3-D object with one down-facing horizontal, one up-facing horizontal and one conical surface. Free convective mass transfer at the truncated cone geometry has not been studied previously. There are few papers on free convective heat transfer at a frustum of a cone (e.g., Na and Chiou, 1979; Koyama et al., 1985). Na and Chiou (1979) reported a numerical solution for the two cases of constant wall temperature and constant wall heat flux. Koyama et al. (1985) performed a theoretical and experimental study to investigate free convection from a vertical frustum of a cone. The experimental investigation was performed only on a single truncated cone.

* Corresponding author. Tel.: +1-392-263656; fax: +1-392-217965.
E-mail address: a.a.wragg@exeter.ac.uk (A.A. Wragg).

0142-727X/02/$ - see front matter
PII: S0142-727X(01)00130-8

Nomenclature

A	surface area, m^2
d_1	diameter of the top base of truncated cone, m (Fig. 2)
d_2	diameter of the bottom base of truncated cone, m (Fig. 2)
c_b	bulk concentration of cupric ions, mol m^{-3}
D	diffusion coefficient of cupric ions, m^2 s^{-1}
F	Faraday constant, 96487 C mol^{-1}
g	gravitational acceleration, m s^{-2}
Gr_L	Grashof number based on inclined surface length, $Gr_L = \Delta\rho g L^3 \rho/\mu^2$
H	height of truncated cone (Fig. 2), m
I_L	limiting diffusion current, A
k	mass transfer coefficient, m s^{-1}
L	length of conical surface of truncated cone, m
L_w	characteristic length defined by Weber et al. (1984), L_w = surface area/perimeter projected onto the horizontal plane, m
n	charge number of cupric ion, $n = 2$
p	pressure, Pa
Pr	Prandtl number
Ra	Rayleigh number, $Ra = GrSc$
$Ra_{L,\theta}$	Rayleigh number based on inclined surface length and on $g\cos\theta$
Sc	Schmidt number, $\mu/\rho D$
Sh	Sherwood number
Sh_L	Sherwood number based on inclined surface length
Sh_d	Sherwood number based on base diameter
T	electrolyte temperature, K

Greek symbols

β	thermal expansion coefficient, K^{-1}
$\Delta\rho$	density difference between bulk solution and interface, kg m^{-3}
ρ	density, kg m^{-3}
μ	dynamic viscosity, kg m^{-1} s^{-1}
θ	inclination angle from the vertical, ° (see Fig. 2)
ν	kinematic viscosity, m^2 s^{-1}

Subscripts

c	conical surface of truncated cone
hd	down-facing horizontal base of truncated cone
hu	up-facing horizontal base of truncated cone
t	total surface of truncated cone

The aim of the present study was:
(a) the measurement of mass transfer rates at the individual surfaces and over the entire surface of various truncated cones (varying length and inclination of conical surface);
(b) to visualise the flow around truncated cones of different heights;
(c) to correlate data taking account of interaction between flow at the individual surfaces.

2. Experimental

The experiments were performed in a rectangular 3 dm^3 optical glass sided container of dimensions 15×30 cm^2 and height 25 cm. The technique used involved the cathodic deposition of cupric ions from a $CuSO_4/H_2SO_4/H_2O$ electrolyte. In order to vary the density difference between bulk fluid and surface the cupric ion concentration was varied from 0.012 to 0.165 mol dm^{-3}. Each solution contained 1.5 mol dm^{-3} sulphuric acid as supporting electrolyte. The electrolyte temperature was carefully measured and always lay within the range 19–22 °C being constant to ±0.1 °C during each individual experiment. The electrodes were machined from solid brass. Each electrode was supported using a 2 mm diameter brass wire glued into a hole in the centre of the horizontal base. This wire also served as a current carrier. The wire was lacquered to insulate it from the electrolyte. The truncated cone cathodes were placed in the centre of the container, in a standard Toepler-schlieren optical system with a camera (see Holder and North, 1963). (Fig. 1). Two copper plates situated either side of the cones served as a counter electrode (anode). The arrangement of the apparatus is similar to that described previously (Krýsa and Wragg, 1996, 1997) and is shown in Fig. 1. The actual Cu^{2+} concentration was periodically determined by spectrophotometric analysis.

The usual electrical circuit for limiting current measurement was employed, consisting of a dc power supply

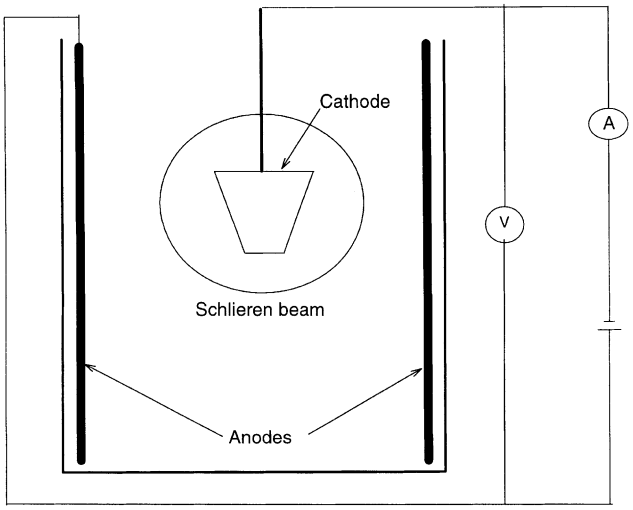

Fig. 1. Apparatus.

with a voltage regulator, a high impedance voltmeter and a multi-range ammeter. Limiting currents were obtained by the well known procedure, which has been reported in detail previously (e.g., Smith and Wragg, 1974). The anode acted as a reference electrode in view of its high area compared to that of the cathode. Under such conditions polarisation is negligible at the anode and the cell current–voltage relationship depends only on the conditions prevailing at the cathode. The onset of the limiting current was sharp and reproducible. In some experiments current transients were recorded by suddenly applying the cathodic limiting current potential. As soon as convection from the edges of the truncated cone was visible schlieren photographs were taken at various stages of flow development and the limiting current was simultaneously recorded.

The geometrical parameters of the truncated cones are illustrated in Fig. 2. Table 1 lists the dimensions used. In this investigation H ranged from 0.2 up to 8.0 cm and θ from $-11°$ up to $-83°$. Inclination angles are counted negative to indicate the down-facing orientation of the conical surface and for consistency with the work of Patrick et al. (1977). The mass transfer controlled limiting currents at the conical surface and at the top and bottom horizontal surfaces were measured separately and also in combination. Surfaces not required to be active were stopped off with lacquer (Lacomit).

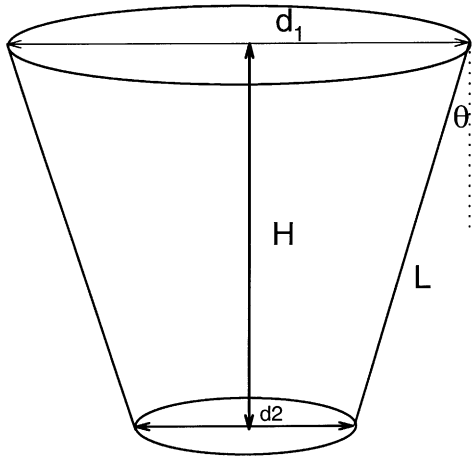

Fig. 2. Geometry of down-pointing truncated cone.

3. Results and discussion

3.1. Mass transfer data calculation

For each experiment the mass transfer coefficient was calculated from the measured limiting current using the equation

$$k = \frac{I_L}{AnFc_b}. \tag{1}$$

The area in this equation was the total available for mass transfer for the particular experiment. The correction for the attachment of the supporting wire was small, never being more than 2% of the exposed area, and usually being much less.

For the conical surfaces the data were expressed in the form of a slant height Sherwood number and a slant height Rayleigh number

$$Ra_{L,\theta} = GrSc\cos\theta = \frac{g\Delta\rho L^3\rho}{\mu^2}\frac{\mu}{\rho D}\cos\theta = \frac{g\Delta\rho L^3}{\mu D}\cos\theta, \tag{2}$$

$$Sh_L = \frac{kL}{D}. \tag{3}$$

The diffusivity of the Cu^{2+} ions was calculated using the data of Wilke et al. (1953). Electrolyte density and viscosity were calculated using data of Eisenberg et al. (1956). The $\Delta\rho$ terms were taken from Wilke et al. (1953). The effect of migration on the copper deposition rate was negligible (see Ibl and Dossenbach, 1983).

Values of Sh_0, the stagnant medium Sherwood number, were subtracted from the overall Sherwood number leaving the convection component of the overall transfer rate. Values of Sh_0 shown in Table 2 were calculated using the method outlined by Clift et al. (1978) according to the equation

Table 1
Geometric parameters of truncated cones

Tr. cone	d_1 (cm)	d_2 (cm)	H (cm)	L (cm)	θ (°)	A_c (cm^2)	A_{hu} (cm^2)	A_{hd} (cm^2)	A_t (cm^2)	d_1/d_2	L_w (cm)
1	3.0	1.0	0.2	1.02	−78.7	6.4	7.1	0.8	14.3	3.0	1.51
2	3.0	0.9	0.5	1.12	−63.4	7.0	6.6	0.7	14.3	3.2	1.52
3	2.9	1.0	1.0	1.42	−45.0	8.9	7.1	0.8	16.7	3.0	1.78
4	3.0	1.0	2.0	2.25	−27.0	14.1	7.1	0.8	22.0	3.0	2.41
5	3.0	1.0	4.0	4.12	−14.0	25.9	7.1	0.8	33.8	3.0	2.35
6	3.0	1.0	8.0	8.06	−7.0	50.6	7.1	0.8	58.5	3.0	6.21
7	3.0	2.0	0.5	0.71	−45.0	5.6	7.1	3.1	15.8	1.5	1.67
8	3.0	0.5	1.25	1.77	−45.0	9.7	7.1	0.2	16.7	6.0	1.77
9	5.0	0.5	2.25	3.18	−45.0	27.5	19.6	0.2	47.3	10.0	3.01

Table 2
Values of Sh_0 (Eq. (4))

Tr. cone	1	2	3	4	5	6
Sh_0	1.94	1.99	2.13	2.48	3.19	4.46

$$Sh_0 = \frac{k_0 L}{D} = \left[8 + 6.95\left(\frac{2L}{d_1 + d_2}\right)\right]. \quad (4)$$

The list of uncertainties in the various measured quantities is given in Table 3. In addition, the uncertainty in the fluid properties D, μ and $\Delta\rho$ was taken as 0.5%. The uncertainty in the determination of the Sherwood number and Rayleigh number depends on the concentration of cupric sulphate solution. For 0.02 mol dm^{-3} it was estimated as 4% and for 0.16 mol dm^{-3} as 1.5%.

3.2. Mass transfer measurement

The effect of the truncated cone height, H, on the mass transfer coefficient for the separate surfaces of truncated cones of constant conical surface inclination (truncated cones 7, 3, 8 and 9) is shown in Fig. 3. The mass transfer rate for the down-facing horizontal base decreases with increase in diameter (from 0.5 to 2.0 cm) which, for constant angle, is related to a decrease in height (from 1.25 to 0.5 cm). The mass transfer rate for the conical surface decreases with increasing height because of the increasing diffusion layer thickness, this being consistent with previous findings for inclined rectangular plates (Patrick et al., 1977) and inclined triangles (Krýsa et al., 1998). The mass transfer rate for a combination of down-facing horizontal surface and conical inclined surface is, for the case of heights of 0.5 and 1 cm, strongly affected by the dominant behaviour of the down-facing horizontal base surface. The down-facing horizontal surface not only has a lower mass transfer performance than the conical surface, but also feeds depleted solution to the 'leading edges' of the conical surface, thus also decreasing its contribution to the combined behaviour. The trend of mass transfer coefficient for conical and combination of conical and down-facing horizontal surfaces with cone height is broadly in agreement with calculations by Koyama et al. (1985) for the case of heat transfer.

Table 3
Uncertainty of measured quantities

Quantity	Nominal value	Uncertainty	Error (%)
D	1.0 cm	0.01 cm	1
H	0.5 cm	0.01 cm	2
H	8.0 cm	0.01 cm	0.13
C_b	0.16 mol dm^{-3}	0.0005 mol dm^{-3}	0.3
C_b	0.02 mol dm^{-3}	0.0005 mol dm^{-3}	2.5
I_L	20 mA cm^{-2}	0.3 mA cm^{-2}	1.5

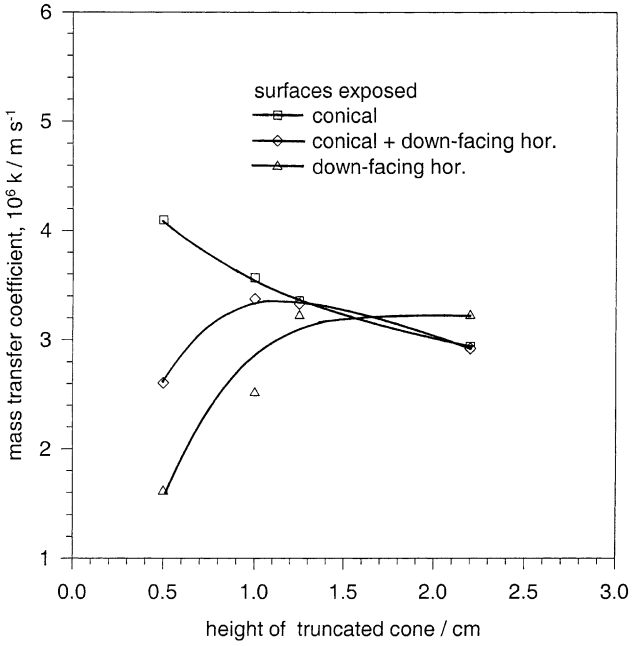

Fig. 3. Effect of truncated cone height on mass transfer coefficient for separate surfaces of truncated cone of constant conical surface inclination for single cupric ion concentration.

The effect of the truncated cone height, h, on the mass transfer coefficient for the separate surfaces of down-pointing truncated cones of constant top (3 cm) and bottom base diameter (1 cm), cones 1–6, is shown in Fig. 4. The superior mass transfer performance of the up-facing horizontal base is immediately apparent,

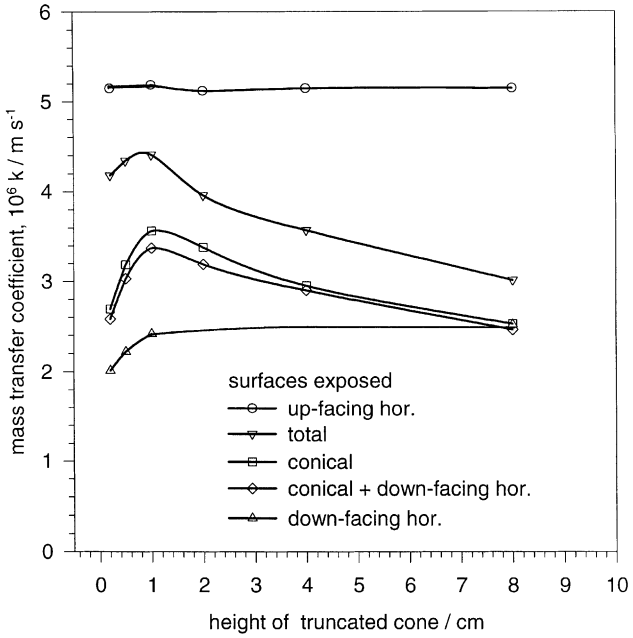

Fig. 4. Effect of truncated cone height on mass transfer coefficient for various surfaces of truncated cone of constant top to bottom diameter ratio for single cupric ion concentration.

especially compared with the down-facing horizontal surface. The mass transfer coefficient for the conical surface initially increases with height (from 0.2 to 1 cm) and then decreases. The presence of the maximum can be explained as follows. The mass transfer coefficient for vertical surfaces (Krýsa and Wragg, 1992; Wilke et al., 1953) and inclined surfaces (constant inclination) (Patrick et al., 1977) decreases with increasing surface length because of the increase in diffusion layer thickness. Therefore the mass transfer coefficient at conical surfaces of constant inclination decreases with inclined length and thus with truncated cone height as was shown in Fig. 3. There is another effect which has to be taken into the consideration – the effect of inclination angle. This produces a decrease in the mass transfer coefficient with decreasing angle of inclination of the down-facing conical surface as demonstrated for rectangular surfaces by Patrick et al. (1977) and for triangular surfaces by Krýsa et al. (1998). Thus, in the case of constant top and bottom base diameters there are two opposed effects on the mass transfer at the conical surface; firstly the truncated cone height and secondly the inclination angle.

The down-facing horizontal base exhibits low mass transfer performance which decreases for truncated cones with heights of 0.5 and 0.2 cm though the base diameter is constant. This behaviour can be explained by considering the effect of the isolated conical surface adjacent to the horizontal base. These have inclinations progressively approaching the horizontal e.g., −63° and −79°, respectively. Thus the behaviour of the down-facing conical surface approaches that of a co-planar collared surface which has recently been shown to have inferior mass transfer performance to that of a surface with free edges (Wragg et al., 1998).

The combined behaviour of the down-facing horizontal base and the conical surface is similar to that of a conical surface alone, the values of mass transfer coefficient being slightly depressed by the performance of the down-facing horizontal surface.

The mass transfer coefficient for the entire surface broadly follows the same behaviour as for the conical surface alone. However, the values are increased by the superior behaviour of the up-facing horizontal base. The increase is especially apparent for truncated cones of heights from 0.2 to 1.0 cm. As for the conical surface alone, the entire truncated cone of 1 cm height shows the highest mass transfer behaviour.

3.3. Flow visualisation

Visualisation of the flow from various truncated cones in 0.165 mol dm^{-3} $CuSO_4$ electrolyte was carried out, schlieren photographs being taken at specific times following sudden switch on of the limiting current potential. The current transients were also simultaneously recorded.

The photographs and transients for the truncated cone with height 1.0 cm are shown in Fig. 5. The tran-

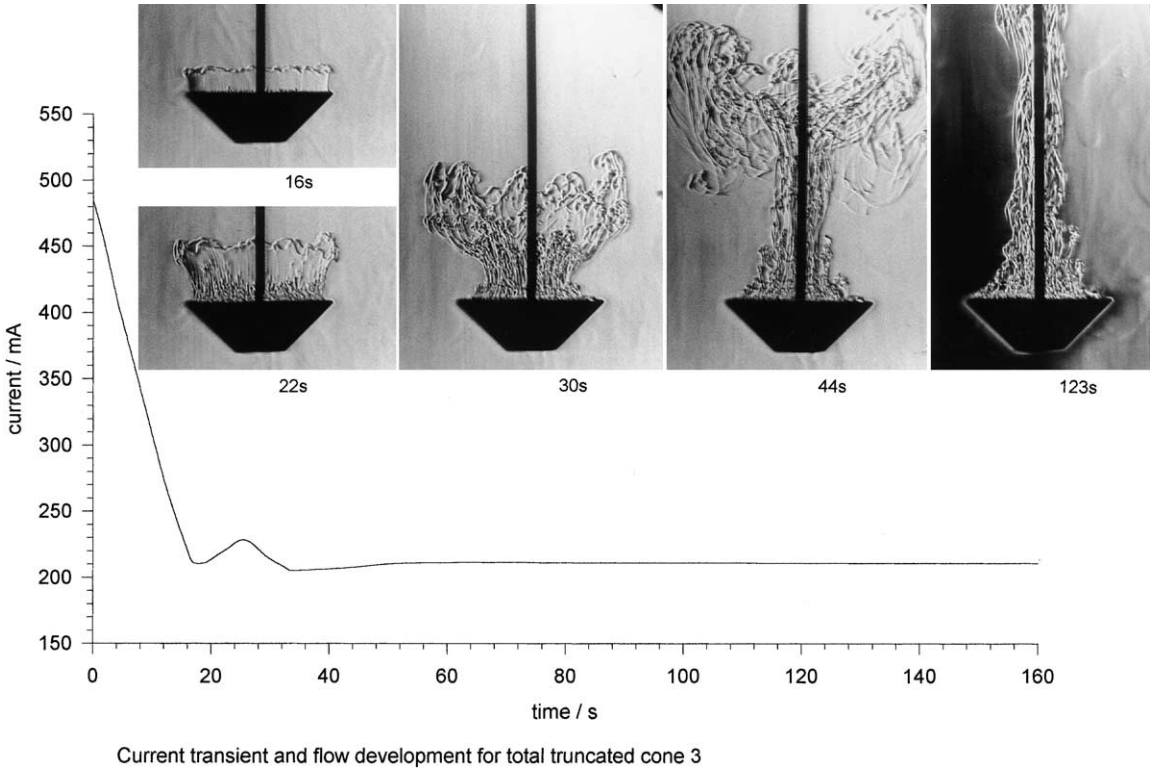

Fig. 5. Current transient and photographs of flow for total truncated cone of height 1 cm (in 0.165 mol dm^{-3} cupric sulphate).

sient is seen to undershoot and then overshoot the eventual steady convective limiting current, a behaviour similar to that observed for up-facing horizontal discs by Patrick and Wragg (1975). Flow begins as a ring of fluid rising from the upper cone periphery. It is notable that convection from the up-facing horizontal base is distinctly visible before the undershoot minimum is reached at about ($t_m = 18$ s). The sharp increase in the mass transfer rate is then caused by the first main generation of convection streams from the up-pointing top which is well established at $t = 30$ s. Necking of the plume then occurs and a steady-state situation arises ($t = 123$ s) in which there is a complex flow structure consisting of a multiplicity of close spaced interacting convection streams; the limiting current is seen to be very steady.

The behaviour of the cone of height 4 cm is shown in Fig. 6. The flow development is similar to that for the cone of height 1 cm; however, the diffusion transient takes significantly longer due to the dominance of the long inclined surfaces not subject to separation. The undershoot and overshoot phenomena are also not visible because of this dominant behaviour of the conical portion of the surface.

Further runs were conducted using truncated cones with inactive tops. Photographs and current transients for a height of 1 cm are shown in Fig. 7. Similarly as for the total truncated cone (Fig. 5) flow begins as a ring of fluid rising around the upper cone periphery. This is followed by the progressive necking and after about 50 s some flow pulsation occurs; this was not observed in the case of the total truncated cone. There is no convection from the isolated up-facing horizontal base and the current–time transient do not exhibit the undershoot and overshoot phenomena typical of horizontal surfaces.

3.4. Overall data correlation

3.4.1. Approach using Weber characteristic dimension

The mass transfer data from entire truncated cones 1–6 are plotted in terms of Sherwood number vs. Raleigh number in Fig. 8 using the characteristic length, L_w, defined previously by Weber et al. (1984). The correlation obtained by Weber et al. for a variety of spherical and non-spherical 3-D objects

$$Sh_{L_w} = Sh_0 + 0.53 Ra_{L_w}^{0.256} \tag{5}$$

is also shown. It is seen that the data from the shorter truncated cones lie under the Weber correlation and the equation is entirely unsuited to the correlation of free convective mass transfer at down-pointing truncated cones. This can be explained by the presence of the down-facing horizontal surface, which not only has a

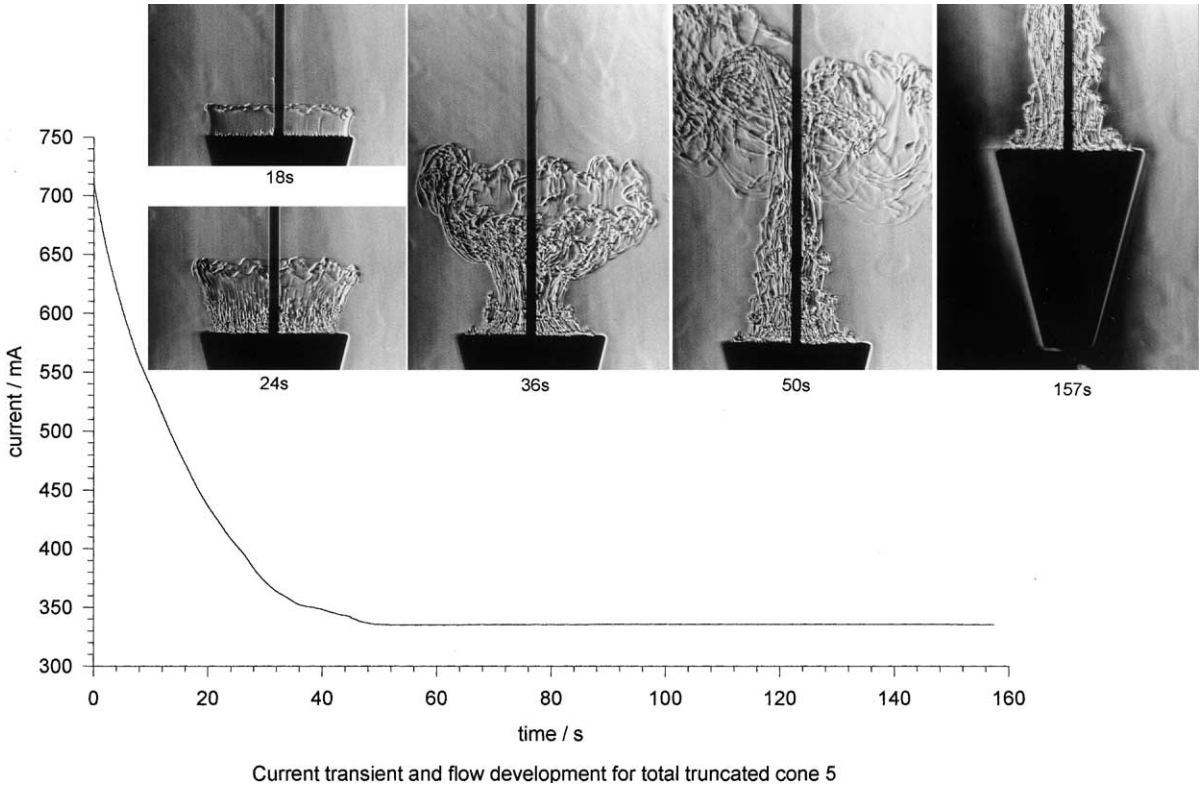

Fig. 6. Current transient and photographs of flow for total truncated cone of height 4 cm (in 0.165 mol dm^{-3} cupric sulphate).

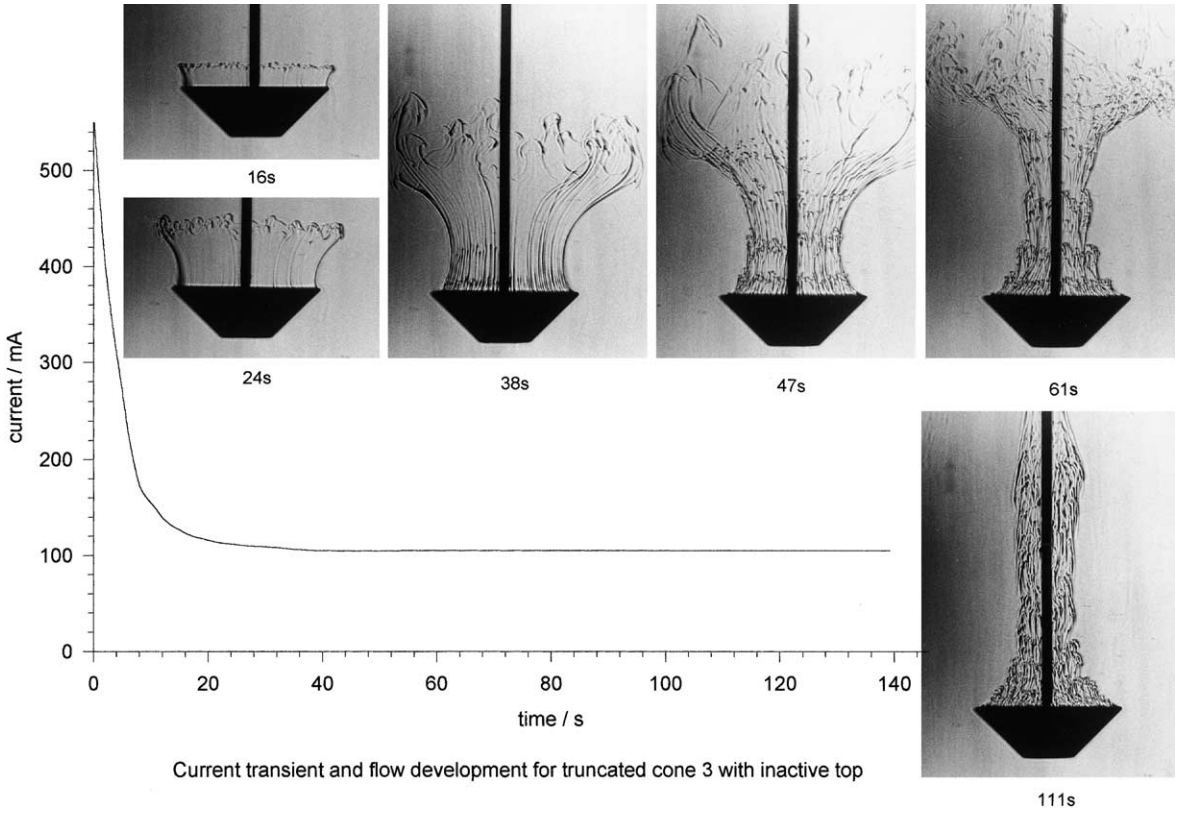

Fig. 7. Current transient and photographs of flow for truncated cone of height 1 cm with inactive top base (in 0.165 mol dm^{-3} cupric).

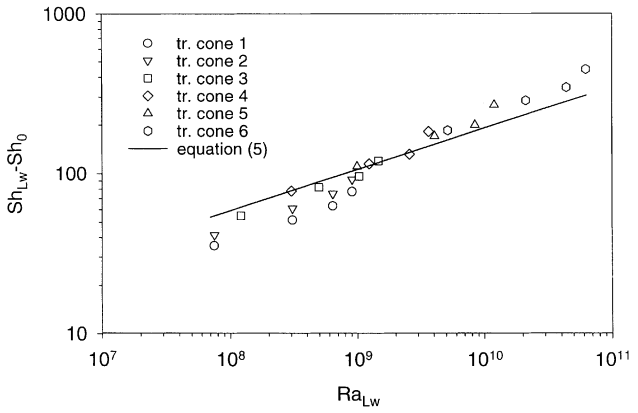

Fig. 8. Correlation of total mass transfer data using the Weber et al. (1984) characteristic dimension.

low mass transfer rate, but also effects flow conditions at the down-facing conical surface thus decreasing the mass transfer rate. The discrepancy with the Weber approach when correlating natural convective mass transfer to cuboids (Worthington et al., 1987), vertical cylinders with active ends (Krýsa and Wragg, 1992), down-pointing and up-pointing pyramids (Krýsa and Wragg, 1996, 1997) has already been reported. Here the Weber correlation is found to be particularly inadequate.

3.4.2. Summation approach to correlation for entire down-pointing truncated cones

By summing the mass transfer rates from correlations for the separate sides a total mass transfer performance can be predicted. The mass transfer correlations for separate surfaces are shown in Fig. 9. In the present approach the correlation for conical surfaces was taken as Eq. (6) (Patrick et al., 1977). For the up-facing horizontal surfaces the correlation was taken as Eq. (7) (Wragg and Loomba, 1970) and for the down-facing horizontal surfaces the correlation was taken as Eq. (8) (Loomba, 1969)

$$Sh_L = 0.68[Ra_L \cos\theta]^{0.25}, \quad (6)$$

$$Sh_d = 0.18Ra_d^{0.33}, \quad (7)$$

$$Sh_d = 0.64Ra_d^{0.22}. \quad (8)$$

The mass transfer rates for separate surfaces were correlated using conical surface length (L) and the horizontal truncated cone base diameter (d) as characteristic lengths. The mass transfer from the whole body comprises mass transfer from the down-facing horizontal surface, the conical surface and the up-facing horizontal surface

$$Sh_t A_t = Sh_{hd} A_{hd} + Sh_c A_c + Sh_{hu} A_{hu}, \quad (9)$$

where Sh_{hd}, Sh_c and Sh_{hu} are Sherwood number for down-facing horizontal, conical and up-facing horizontal

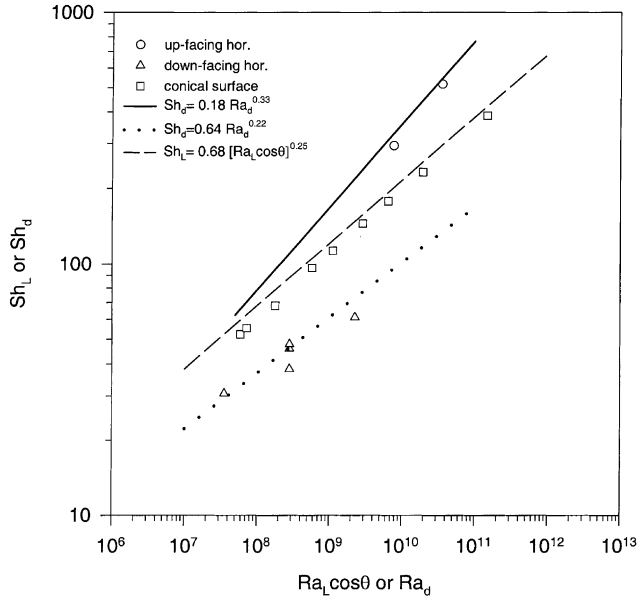

Fig. 9. Mass transfer correlations for single separate surfaces of truncated cone.

surface, respectively. Introducing correlations (6)–(8) into Eq. (9), evaluating total (A_t) and separate surface areas ($A_{hd} = \pi d_2^2/4$, $A_c = (d_1 + d_2)\pi L/2$ and $A_{hu} = \pi d_1^2/4$) and rearranging we obtain the resultant predicted natural convection mass transfer rate for down-pointing truncated cones

$$Sh_L - Sh_0 = \left\{ \left[(0.64(d_2)^2\ Ra^{-0.03} + 1.36(d_1 + d_2) \times \sqrt{L^2 - \tfrac{1}{4}(d_1 - d_2)^2} + 0.18(d_1)^2 Ra^{1/12} \right] \Big/ \left[(d_1)^2 + (d_2)^2 + 2(d_1 + d_2)L \right] \right\} Ra_L^{0.25}, \tag{10}$$

where L is the length of conical surface and d_1 and d_2 are the top and bottom horizontal diameters, respectively, and Ra_L is a Rayleigh number based on the conical surface length.

3.4.3. Summation approach with interference

The behaviour predicted by Eq. (10) was compared with the mass transfer data for truncated cones. It was found in every case that the predicted rate was about 5–25% higher than the actual. The flow of the fluid around the down-facing horizontal base means that the conical and up-facing horizontal surfaces are exposed to solution which has already been depleted of cupric ions. This boundary layer spillover effect causes the overall mass transfer for a truncated cone to be lower than that for the equivalent summed separate surfaces. A multiplying factor, f (an interference factor), may be introduced to Eq. (10) to represent the lower rate of mass transfer at conical and up-facing horizontal surfaces. Eq. (10) now becomes

$$Sh_L - Sh_0 = \left\{ \left[0.64(d_2)^2\ Ra^{-0.03} + f\left(1.36(d_1 + d_2) \times \sqrt{L^2 - \tfrac{1}{4}(d_1 - d_2)^2} + 0.18(d_1)^2 Ra^{1/12} \right) \right] \Big/ \left[(d_1)^2 + (d_2)^2 + 2(d_1 + d_2)L \right] \right\} Ra_L^{0.25}. \tag{11}$$

As a first step the applicability of correlating Eq. (11) was tested using the set of cones 1–6. These cones have constant top and bottom diameter and therefore only the conical surface length and inclination affects the value of f. The averaged values of f obtained from Eq. (11) are tabulated in Table 4. $Sh_L - Sh_0$ has been plotted to show the data from truncated cones of constant top to bottom diameter ratio against $\Phi(L, d_1, d_2, Ra_L)Ra_L$ in Fig. 10. Here $\Phi(L, d_1, d_2, Ra_L)$ is given by

$$\Phi(L,d_1,d_2,Ra_L) = \left[\left\{ 0.64(d_2)^2\, Ra^{-0.03} + f\left(1.36(d_1+d_2) \times \sqrt{L^2 - \tfrac{1}{4}(d_1 - d_2)^2} + 0.18(d_1)^2 Ra^{1/12} \right) \right\} \Big/ \left\{ (d_1)^2 + (d_2)^2 + 2(d_1+d_2)L \right\} \right]^4. \tag{12}$$

It can be seen that the data from truncated cones fit the line representing equation (11) well and the fit is far better than that of the Weber correlation based on a single characteristic length. The interference factor, f

Table 4
Dependence of interference factor, f, on geometry of down-pointing truncated cone

Tr. Cone	1	2	3	4	5	6
f	0.97	0.89	0.83	0.81	0.81	0.82

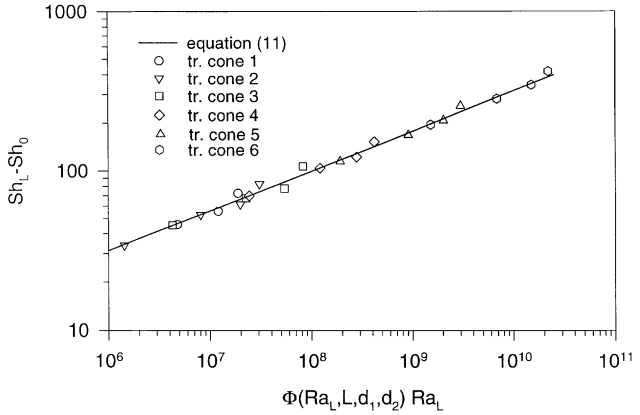

Fig. 10. Overall data correlation for entire truncated cones of constant top to bottom diameter ratio (1–6) in terms of Eq. (12).

(Table 4) decreases with the L/d_2 ratio and for L/d_2 values in the range from 2 to 8, f is approximately constant. The correlating equation (11) cannot be applied generally to all possible examples of truncated cones. The effect of cone geometry on the values of interference factor is complex and deserves further study. The universality of the separate side correlation approach will be further tested on truncated cones of more varied geometry.

4. Conclusions

(i) The superior mass transfer performance of the up-facing horizontal surface was observed especially compared with the down-facing horizontal surface.
(ii) The dependence of total mass transfer on cone height broadly follows the same behaviour as that for conical surfaces, i.e., exhibits a maximum due to the two opposed effects of truncated cone height and inclination angle.
(iii) Flow visualisation shows that the steady plume consists of a multiplicity of close placed interacting streams. The long inclined cone surface is not subject to separation disturbances.
(iv) The separate side correlation approach was used to correlate the experimental total mass transfer data. An interference factor taking account of the fact that the conical and up-facing horizontal surfaces of the truncated cones are exposed to fluid which has already been depleted in cupric ions has been introduced in producing a satisfactory correlating equation. Values of the interference factor, f, have been determined.

Acknowledgements

The present study was supported by the project MSM 223100001. Financial support from the Royal Society for a visit to Exeter by J.K. is also gratefully acknowledged.

References

Clift, R., Grace, J.R., Weber, M.E., 1978. In: Bubbles and Drops and Particles. Academic Press, New York, pp. 88–91.

Eisenberg, M., Tobias, C.W., Wilke, C.R., 1956. Selected properties of ternary electrolytes employed in ionic mass transfer studies. J. Electrochem. Soc. 103, 413–416.

Holder, D.W., North, R.J., 1963. Schlieren Methods, Notes on Applied Science No. 31, National Physical Laboratory, London.

Ibl, N., Dossenbach, O., 1983. In: Yeager, E., Bockris, J.O' M., Conway, B.E., Sarangapani, S. (Eds.), Comprehensive Treatise of Electrochemistry, vol. 6. Plenum Press, New York, pp. 192–198.

Koyama, H., Nakyama, A., Ohsawa, S., Yamada, H., 1985. Theoretical and experimental study of free convection from a frustum of a cone of a finite length. Int. J. Heat Mass Transfer 28, 969–976.

Krýsa, J., Wragg, A.A., 1992. Free convection mass transfer at vertical cylindrical electrodes with varying aspect ratio. J. Appl. Electrochem. 22, 429–436.

Krýsa, J., Wragg, A.A., 1996. Free convection mass transfer at down-pointing pyramidal electrodes. Int. J. Heat Mass Transfer 39, 1297–1305.

Krýsa, J., Wragg, A.A., 1997. Free convection mass transfer at up-pointing pyramidal electrodes. Int. J. Heat Mass Transfer 40, 3717–3727.

Krýsa, J., Iino, F., Wragg, A.A., 1998. Free convective mass transfer at down-pointing isosceles triangles of varying inclination. Coll. Czech. Chem. Com. 63, 2114–2122.

Loomba, R.P., 1969. Free convection mass transfer at horizontal surfaces, M.Sc. Thesis, University of Manchester.

Na, T.Y., Chiou, J.P., 1979. Laminar natural convection over a frustum of a cone. Appl. Sci. Res. 35, 409–421.

Patrick, M.A., Wragg, A.A., 1975. Optical and electrochemical studies of transient free convection mass transfer at horizontal surfaces. Int. J. Heat Mass Transfer 18, 1397–1407.

Patrick, M.A., Wragg, A.A., 1985. Modelling of free convection in heat transfer using electrochemical mass transfer techniques. I. Chem. Eng. Symp. Series 94, 45–55.

Patrick, M.A., Wragg, A.A, Pargeter, D.M, 1977. Mass transfer by free convection during electrolysis at inclined electrodes. Can. J. Chem. Eng. 55, 432–438.

Smith, A.F.J., Wragg, A.A., 1974. An electrochemical study of mass transfer in free convection at vertical arrays of horizontal cylinders. J. Appl. Electrochem. 4, 219–228.

Weber, M.E., Austraukas, P., Petsalis, S., 1984. Natural convection mass transfer to nonspherical objects at high Rayleigh number. Can. J. Chem. Eng. 62, 68–72.

Wilke, C.R., Tobias, C.W., Eisenberg, M., 1953. Correlation of limiting currents under free convective condition. J. Electrochem. Soc. 100, 513–517.

Worthington, D.R.E., Patrick, M.A., Wragg, A.A., 1987. Effect of shape on natural convection heat and mass transfer at horizontally oriented cuboids. Chem. Eng. Res. Des. 65, 131–138.

Wragg, A.A., Loomba, R.P., 1970. Free convection at horizontal surfaces with ionic mass transfer. Int. J. Heat Mass Transfer 13, 439–442.

Wragg, A.A., Batting, G., Krýsa, J., 1998. Free convective mass transfer at down-facing horizontal surfaces with free or collared edges. Int. Comm. Heat Mass Transfer 25, 175–182.